Dalton Transactions

Accepted Manuscript

This is an *Accepted Manuscript*, which has been through the RSC Publishing peer review process and has been accepted for publication.

Accepted Manuscripts are published online shortly after acceptance, which is prior to technical editing, formatting and proof reading. This free service from RSC Publishing allows authors to make their results available to the community, in citable form, before publication of the edited article. This *Accepted Manuscript* will be replaced by the edited and formatted *Advance Article* as soon as this is available.

To cite this manuscript please use its permanent Digital Object Identifier (DOI®), which is identical for all formats of publication.

More information about *Accepted Manuscripts* can be found in the **Information for Authors**.

Please note that technical editing may introduce minor changes to the text and/or graphics contained in the manuscript submitted by the author(s) which may alter content, and that the standard **Terms & Conditions** and the **ethical guidelines** that apply to the journal are still applicable. In no event shall the RSC be held responsible for any errors or omissions in these *Accepted Manuscript* manuscripts or any consequences arising from the use of any information contained in them.

RSC Publishing

www.rsc.org/dalton
Registered Charity Number 207890

ARTICLE TYPE www.rsc.org/xxxxxx | XXXXXXXX

View Online

Synthesis, Structures of (Aminopyridine)nickel Complexes and Their Use for Catalytic Ethylene Polymerization

Ya-Chi Lin, Kuo-Hsuan Yu, Ya-Fan Lin, Gene-Hsiang Lee, Yu Wang, Shiuh-Tzung Liu and Jwu-Ting Chen*

Received (in XXX, XXX) 1st January 2007, Accepted 1st January 2007
First published on the web 1st January 2007
DOI: 10.1039/b000000x

A series of α-aminopyridines in the form of (2,6-C_6H_3N)(R^1)($CHR^2NR^3R^4$) (R^1 = R^2 = H R^3 = H R^4 = ^{i}Pr (**L1a**), R^4 = ^{t}Bu (**L1b**), R^4 = Ph (**L1c**), R^4 = 2,6-$Me_2C_6H_3$ (**L1d**), R^4 = 2,6-$^i Pr_2C_6H_3$ (**L1e**), R^1 = R^2 = H R^3 = R^4 = Et (**L1f**), R^1 = H R^2 = Me R^3 = H R^4 = ^{i}Pr (**L2a**), R^4 = Ph (**L2c**), R^4 = 2,6-$Me_2C_6H_3$ (**L2d**), R^4 = 2,6-$^i Pr_2C_6H_3$ (**L2e**), R^1 = Me R^2 = H R^3 = H R^4 = 2,6-$^i Pr_2C_6H_3$ (**L3e**)) and β-aminopyridines in the form of (2-C_6H_4N)($CH_2CH_2NR^1R^2$) (R^1 = H R^2 = ^{i}Pr (**4a**), R^2 = ^{t}Bu (**L4b**), R^1 = R^2 = Et (**L4f**)) have been prepared. Their corresponding halonickel complexes **1a**~**4f** are synthesized by ligand substitution from (DME)$NiBr_2$ and the molecular structures are characterized. Four types of coordination modes include four-coordinate mononuclear species with one ligand, five-coordinate mononuclear species with two ligands, five-coordinate dinuclear species with two ligands, and a six-coordinate polymeric framework were determined by X-ray crystallography. Using methylaluminoxanes (MAO) as the activator, the nickel complexes can catalyze ethylene polymerization under moderate pressure and ambient temperature. The activity reaches to 10^5 g PE/mol Ni·h. The PE products of high branches and high crystallinity have M_n~10^3 with PDI<2.

Introduction

Late transition metal catalyzed ethylene polymerization have been attracting tremendous research attention in the latest decade.[1] An intriguing aspect in such reactions is that variation of molecular catalysts, particularly with fine-tune in the ligands, may lead to profound electronic and steric control to the reaction activity as well as the property of the macromolecular products.[2]

We have previously found that dibromonickel complexes bearing hemi-labile bidentate *α*-aminoaldimines can catalyze the formation of hyperbranching PE.[3] Along this research line, we prepared more than a dozen derivatives of *α*- and *β*-aminopyridines which are also of the combination of sp^2- and sp^3-nitrogen donor atoms, like the previously studied aminoaldimines, but with aromatic ring skeleton. We also prepared their nickel(II) complexes that exhibit variation in structural features. Upon the activation by methylaluminoxanes (MAO), the (aminopyridine)halonickel(II) complexes are found to catalyze ethylene polymerization that yields fibrous PE of low molecular weight.[4]

Results and Discussion

Synthesis of Aminopyridine and Their Nickel Complexes

The *α*-aminopyridines in the form of (2,6-C_6H_3N)(R^1)(CHR^2-NR^3R^4) (R^1 = R^2 = H R^3 = H R^4 = ^{i}Pr (**L1a**), R^4 = ^{t}Bu (**L1b**), R^4 = Ph (**L1c**), R^4 = 2,6-$Me_2C_6H_3$ (**L1d**), R^4 = 2,6-$^i Pr_2C_6H_3$ (**L1e**), R^1 = H R^2 = Me R^3 = H R^4 = ^{i}Pr (**L2a**), R^4 = Ph (**L2c**), R^4 = 2,6-$Me_2C_6H_3$ (**L2d**), R^4 = 2,6-$^i Pr_2C_6H_3$ (**L2e**), R^1 = Me R^2 = H R^3 = H R^4 = 2,6-$^i Pr_2C_6H_3$ (**L3e**)) were prepared via condensation with equimolar amine and 2-pyridine-carboxaldehyde or 2-acetylpyridine catalyzed by acid, and ensuing reduction using $NaBH_4$ under mild conditions. (2-C_6H_4N)CH_2NEt_2 (**L1f**) was obtained by means of direct reductive amination[5,6] (Scheme 1).

Scheme 1 Synthesis of *α*-aminopyridines

<Scheme 1 here>

β-Aminopyridines in the form of (2-C_6H_4N)($CH_2CH_2NR^1R^2$) (R^1 = H R^2 = ^{i}Pr (**L4a**), R^2 = ^{t}Bu (**L4b**), R^1 = R^2 = Et (**L4f**)) were prepared first via tosylation of 2-(2-hydroxyethyl)pyridine and successive replacement of amine for tosylate (Scheme 2).[7] Characterization for the ligands was mainly carried out by NMR techniques.

Scheme 2 Synthesis of *β*-aminopyridines

<Scheme 2 here>

As previously reported procedures for other bromonickel(II) complexes, the corresponding complexes with the fourteen

aminopyridines, designated as **1a**~**1f**, **2a**~**2e, 3e, 4a**, **4b**, and **4f**, were readily obtained by the substitution reactions with equimolar amounts of the ligands and (DME)$NiBr_2$ (DME = 1,2-dimethoxyethane).[4] All products are paramagnetic. The SQUID measurements for **1d, 1e, 1f**, **2d** and **3e**, provide the values for μ_{eff} are 3.69, 4.00, 2.39, 3.55 and 4.52 BM, respectively, indicating that **1f** has two unpaired electrons; and **1d, 1e, 2d** and **3e** have four unpaired electrons, which are in agreement with the dinuclear structures as illustrated in next session. Similar reactions of (DME)$NiBr_2$ and **L1a**, **L1b**, or **L1d** in stoichiometric ratio of 1:2 produce air-stable complexes **1a'**, **1b'**, or **1d'**, respectively.

X-ray Structural Analysis

Recrystallization of the nickel complexes was carried out in CH_2Cl_2-Et_2O co-solvents. The single crystals suitable for X-ray diffractions are analyzed by crystallography. The results allowed us to further understand the coordination style of aminopyridines in Ni(II) complexes.[4] Unlike (diimine)$NiBr_2$ and (aminoaldimine)$NiBr_2$ which are in tetrahedral,[8,3] and an (aminopyridine)$_2NiBr_2$ complex is found in octahedral,[4] we have observed four types of molecular configurations for the investigated species, including four-coordinate mononuclear, five-coordinate dinuclear,[9] five-coordinate mononuclear,[10] and six-coordinate polymeric molds.[11]

The four-coordinate mononuclear species, **1f**, **4b**, and **4f** all show distorted tetrahedral geometry. Figure (1a) displays the ORTEP drawing of **4b** as a representative. The lengths of the Ni-N_{am} bonds are in the range of 2.036(3)-2.044(3) Å and 1.979(3)-1.991(3) Å for Ni-N_{py} bonds. The N_{am}-Ni-N_{py} angle is 84° for **1f**, but in the larger range of 97-99° for **4b** and **4f** respectively.

Complexes **1d**, **1e**, **2d**, **2e**, **3e** and **4a** have two trigonal bipyramidal nickel centers bridged by a pair of bromide. The ORTEP for **1e** is shown in Figure (1b) as the representative. The bridging bromides show longer distances to the nickel center. The axial one trans to pyridinyl nitrogen, Ni1-Br1, is 2.4882(5) and the equitorial one, Ni1-Br1A, is 2.5512(5) Å. The terminal bromide that take the equatorial site is closer to the nickel, with Ni1-Br2 being 2.4229(5) Å. Such a configuration is supposed to be formed from dimerization of two four-coordinate units as in Figure (1a).

Complex **2a** is found in a six coordinate polmeric network as shown in Figure 1(c). In it's unit cell, two nickel centers are linked with two bridging bromides, resulting in the distance of Ni-Ni being 3.949 Å. The N1-Ni-N2 angle is 80.21(9). The trans basal angles (N(1)-Ni-Br(1) 167.16(7)° and N(2)-Ni-Br(2) 178.58(6)°) and the sum of the angles at Ni (359.92°) are in good agreement with this geometry. The Ni center disposes 0.057 Å out of the plane N1-N2-Br1-Br2. The lengths of Ni-Br1 and Ni-Br2 that are trans to N1 and N2 are 2.5958(4) and 2.6052(4) Å; and the lengths of other two axial bonds Ni-Br1A, Ni-Br2B are 2.6221(4), 2.6087(4) Å, respectively.

The molar ratios between ligand and metal in the cationic complexes **1a'**, **1b'** and **1d'** are all in 2:1. The ORTEP of

Figure 1 ORTEP drawings of (a) [^{t}BuHNCH$_2$CH$_2$(*o*-C_6H_4N)]-$NiBr_2$ (**4b**), (b) {[*o*-^{i}Pr$_2C_6H_3$NCH$_2$(*o*-C_6H_4N)]$NiBr_2$} (**1e**), (c) {[^{i}PrHNCHMe(*o*-C_6H_4N)]$NiBr_2$}$_n$ (**2a**), (d) {[*o*-$Me_2C_6H_3$NH-CH_2(*o*-C_6H_4N)]$_2NiBr$}Br (**1d'**) all hydrogen atoms are omitted.

(a)

< Figure 1(a) here >

(b)

< Figure 1(b) here >

(c)

< Figure 1(c) here >

(d)

< Figure 1(d) here >

five-coordinate **1d'** in slightly distorted triginal bipyramidal configuration is shown in Figure 1(d) as a representative. The nitrogen atoms of two pyridine occupy the axial positions with the angle of N1-Ni-N3 being 172.7(1)°. And, two amino nitrogen atoms and the terminal bromine atom constitute the equitorial trigonal plane, that is evidenced by the sum of the angles N2-Ni-Br1, N4-Ni-Br1, and N4-Ni-N2 being nearly 360°.

Figure 2 Various structural configurations of the (amino-pyridine)nickel complexes.

<Figure 2 here>

In a general view, such variation of solid state structures for the aminopyridine-ligated nickel bromides suggests that there may be dynamic equilibria among these species in the solutions. The plausible reactions may involve four-coordinate mononuclear complex as the form **A** in Figure 2. Complex **A** can either undergo dimerization to yield the doubly bromide-bridged dinickel species **B**, or convert to the cationic **D** by addition of extra aminopyridine. The dinuclear complex **B** can generate six-coordinate polymeric **C** via further successive combination reactions.

Ethylene Polymerization

Ethylene polymerization has been found to be resulted with use of the complexes of aminopyridinenickel bromides with the assistance of methylaluminoxane (MAO) as the activator. In the typical runs, into a 600 mL stainless-steel autoclave, 21 μmol nickel catalyst and 430 molar equivalents of MAO were first placed in toluene. Then ethylene was charged to a pressure of 17 bar. The reaction solution was magnetically stirred at 25 □. The reaction temperature was substantially increased upon the reaction course due to the highly exothermal process of polymerization.

After the desired time, the reaction was terminated by addition of acidified methanol. White solid polyethylenes were collected and characterized. The results are summarized in Table 1. The yields are varied from poor to very good. The activities of the catalysts were evaluated as 10^2~10^5 g(PE)/mol(Ni)·h, except for the reaction of complex **1c** and **2a** from which only oligomers were resulted.

The molecular weights of PE products are in the range of 10^3 with dispersity generally below 2.0, but the results from **4f** reaching to 4.0. Although with such low molecular weights, the solubility of the resulting polymers in toluene is poor, indicating that the crystallinity of the PE may be high.

Ligand Effect on Catalyst Activity and Polymer Properties

The activity of the catalyst is significanly dependent on the ligand. Among the data for precursors **1a**~**1e**, the activity toward ethylene polymerization appears to be increasing with the steric bulkiness of the amino substituent. Complexes **1d** or **1e** with the ortho-substituted aryl at the amino nitrogen shows particularly good activity. Such a trend is basically in

Table 1 Data of ethylene polymerizations catalyzed by (aminopyridine)nickel bromides with MAO[a]

Catalyst (μmol)	MAO (mmol/equiv)	Yield (g)	Activity[c] (kg·mol^{-1}h^{-1})	Mn[d] (× 10^3)	PDI[d]	Branches/ 1000C[e]	T_g[f]	T_m[f]
1a (21.7)	8.74 / 403	0.05	1.15	1.21 203	1.5 1.9	75	53	119
1b (21.0)	8.74 / 416	0.10	2.38	1.76	1.7	44	50	119
1c (20.0)	8.74 / 437	0.39	9.75	0.46	1.5	65	n. d.[g]	77, 116
1d (20.8)	8.74 / 420	5.37	129	2.47	2.2	78	43	117
1e (20.5)	8.74 / 426	18.86	460	1.26	1.9	44	46	114
1f (20.9)	8.74 / 418	0.03	0.77	1.10 96	3.5 1.8	112	45	126
2a (20.9)	8.74 / 418	31.44	752	0.40	1.9	115	n. d.[g]	n. d.[g]
2c (21.6)	8.74 / 405	2.10	49	1.23	1.4	77	n. d.[g]	n. d.[g]
2d (20.3)	8.74 / 431	18.63	459	1.98	3.2	68	28	115
2e (20.0)	8.74 / 437	8.76	219	6.87	1.4	72	44	n. d.[g]
3e (20.0)	8.74 / 437	0.15	3.75	n. d.[g]	n. d.[g]	88	27	119
4a (21.0)	8.74 / 416	0.07	1.67	2.55	1.4	96	52	120
4b (20.2)	8.74 / 433	0.06	1.39	n.d.[g]	n. d.[g]	131	45	123
4f (20.1)	8.74 / 435	0.01	0.30	16.4	4.0	71	45	121, 129
1a' (20.0)[b]	8.74 / 437	0.61	2.77	0.37 196	1.2 1.2	174	45	92

[a] Reaction conditions: 17 bar of ethylene, 50 mL of toluene, 2h, room temperature. [b] Reaction time = 11 h. [c] One experiment run was performed for each catalyst. [d] Determined by GPC using polystyrene as standards. [e] Methyl branches per 1000 carbons; determined by ^{1}H NMR spectroscopy. [f] Determined by DSC. [g] n.d. = not detected.

agreement with other precedented cases in which the chelated ligands of nitrogen donor atoms such as diimines[8a,12] or α-aminoaldimines were used.[3] It is attributed to that the steric bulkiness in the ligands as the ortho-disubstituted aryl groups can destabilize the ethylene-coordinated state, thus facilitate the ethylene insertion.[8a]

The most noticeable activity enhancement for the title catalysts is shown by **2a**~**2e**, is the methyl substituent at the α-carbon of α-aminopyridines. We believe that the steric hindrance within the ligand between the methyl group in the backbone and the adjacent amino substituent may enhance the steric control toward the reactions.

In addition, by comparison with the previous studies on the (α-aminoaldimine)nickel bromides,[3] these α-aminopyridine complexes can give equal activity, dispersity, but much lower molecular weights and relatively lower branching numbers. In one run using [2-C_6H_4NCH=N(2,6-$^iPr_2C_6H_3$)]$NiBr_2$ as the precursor, an activity with one order of magnitude higher than that resulting from **1e** was acquired under the similar conditions.[13]

Apparently, the stronger donating group as 2,6-$^iPr_2C_6H_3$ can facilitate the ethylene insertion at the nickel center either in imine or amine. This is also supported by the higher activity resulting from **1a'** which bears two ligands than in **1a.** However, the low molecular weights indicate that the amino-pyridines may lead to poor steric control around the metal, thus lose the control to the chain transfer than those precursors with diimines or α-aminoaldimines can do.

Reaction conditions and polymerization

In contrary to the previous results from the diimine cases,[8a] the TOF of polymerization is found to be linearly dependent on the pressure of ethylene in the range of 14 to 21 bar as shown in the entries 1-3 of Table 2. In the mean time, the branching number also increases. However, the values of M_n and PDI hardly change. We suggest that the rate-determining step in such reactions should be at the ethylene coordination instead of ethylene insertion. The resting state is likely the Ni(alkyl) cation instead of the Ni(alkyl)(C_2H_4) cation. Thus, the high ethylene concentration assists ethylene coordination, and maybe chain-walking too, but not β-H elimination.

The growing viscosity of the product polymers can hinder the polymerization during the reaction course. Entries 4-7 of Table 2 show that the activity increases while larger amount of toluene is employed. In the meantime, the values of Mn, PDI, and the branching number are also somewhat raised up. This may be due to that the heat dissipation is more effective in dilute conditions and allow longer lifetime for the catalysts.

In Table 3, entries 1-5 show the increase of yields from 15-240 min at 24 °C. Such results indicate that the catalyst is stable and keep steady activity under mild temperature. In fact, entries 2 and 6-9 show that the catalyst **1e** gives the best activity at 35 °C at [Al]/[Ni] = 426.

The use of MAO is critical to the polymerization. Entries 2 and 10-13 in Table 3 exhibit that the yield of PE increases by varying the ratio of [Al]/[Ni] in the range of 256 to 767, then drops from 767 to 1023. Large amount of MAO contains too much trialkylaluminum that may result in catalyst degradation.[14]

As the temperature is raised over 35 °C, neither the ethylene solubility nor the catalyst stability will be favored for the polymerization. The polymer obtained at 70 °C can dissolve in toluene completely. In contrast, the product obtained at 1.5 °C is not soluble in toluene at all, which may be attributed to its high crystallinity. The crystallinity of PE product obtained at 1.5 °C is further supported by the data of powder X-ray diffraction, DSC and SEM techniques. In powder X-ray diffraction, it is noted that the spikes of the orthorhombic (110) and (200) with respect to 2θ move to the left from 24 °C to 50 °C. These changes indicate the average crystallite sizes increase from 110, 70 Å to 125, 105 Å, respectively.[15] At 1.5 °C, the broad noncrystalline hump between 15-25 degrees nearly disappears (see supporting information Figure S6).

Unlike the PE yielded at 24-70 °C, which show low T_g and T_m in the range of 114-105 °C in their DSC curves, the PE resulted at 1.5 °C have a single peak at 126 °C, suggesting a non-entangled high ordering crystal phase. The SEM images for the PE confirm such results. As shown in Figure 3, the PE catalyzed by **1e** at 70 °C is highly amorphous, while at 1.5 °C, the PEs appear in fibrous crystalline.

In conclusion, dibromonickel catalysts that bear bidentate ligands of aminopyridine, showing four-, five-, or six-coordinate mononuclear, dinuclear, and polymeric configurations in solid state, are effective polymerization of ethylene with the assistance of MAO, yielding PE with fibrous crystallinity.

Table 2 Ethylene pressure and dilution effects on polymerization catalyzed by **2d** with MAO

Entry	Ethylene (Bar)	Toluene (mL)	Yield (g)	Activity ($kg \cdot mol^{-1}h^{-1}$)	Mn[c] ($\times 10^{-3}$)	PDI[c]	Branches/ 1000C[d]	T_g[e]	T_m[e]
1[a]	14	50	0.64	4.86	0.98	1.3	39	n. d.[f]	n. d.[f]
2[a]	17	50	1.40	8.40	1.10	1.3	58	n. d.[f]	n. d.[f]
3[a]	21	50	2.90	14.52	0.70	1.5	62	n. d.[f]	n. d.[f]
4[b]	17	50	18.63	459	1.98	3.2	68	26	115, 121
5[b]	17	100	19.11	470	8.76	1.4	46	26	108
6[b]	17	150	21.51	603	2.21	3.5	80	23	111, 119
7[b]	17	200	30.63	754	2.90	3.0	70	24	113, 120

[a] Reaction conditions: 19.2 μmol of **2d**, 455 equiv. of MAO, 30 min, room temperature. [b] Reaction conditions: 20.3 μmol of **2d**, 431 equiv. of MAO, 120 min, room temperature. [c] Determined by GPC using polystyrene as standards. [d] Methyl branches per 1000 carbons; determined by ^1H NMR spectroscopy. [e] Determined by DSC. [f] n. d. = not detected.

Table 3 Ethylene polymerizations catalyzed by **1e** with MAO[a]

Entry	MAO (mmol/equiv)	Time (min)	Temp. (°C)	Yield (g)	Activity (kg·mol^{-1}h^{-1})	Mn[b] (× 10^{-3})	PDI[b]	Branches/ 1000C[c]	T_g[d]	T_m[d]
1	8.74 / 426	15	24	2.66	519	1.76	1.6	68	n. d.[e]	n. d.[e]
2	8.74 / 426	30	24	3.55	346	1.95	1.8	47	27	114
3	8.74 / 426	60	24	7.27	355	1.39	1.7	33	24	104
4	8.74 / 426	120	24	18.86	460	1.26	1.9	44	46	114
5	8.74 / 426	240	24	28.04	342	0.98	2.1	63	n. d.[e]	114
6	8.74 / 426	30	1.5	1.09	167	n. d.[e]	n. d.[e]	n. d.[e]	96	126
7	8.74 / 426	30	35	8.64	843	1.12	1.8	69	27	107
8	8.74 / 426	30	50	2.09	204	1.54	1.6	84	n. d.[e]	105
9	8.74 / 426	30	70	0.19	19	1.83	1.3	76	n. d.[e]	n. d.[e]
10	8.74 / 256	30	24	2.21	216	2.38	1.5	91	18	113
11	8.74 / 597	30	24	9.13	891	1.04	7.9	45	15	110
12	8.74 / 767	30	24	10.18	993	1.14	2.0	51	29	108
13	8.74 / 1023	30	24	6.86	669	1.13	2.4	41	n. d.[e]	117

[a] Reaction conditions: 20.5 μmol of **1e**, 17 bar of ethylene, 50 mL toluene. [b] Determined by GPC using polystyrene as standards. [c] Methyl branches per 1000 carbons; determined by ^{1}H NMR spectroscopy. [d] Determined by DSC. [e] n. d. = not detected.

Figure 3 SEM image of PE produced by **1e** at (a) 70 (b)1.5 ℃. (a)

<Figure 3 (a) here>

(b)

<Figure 3 (b) here>

Experimental Section

General Procedures

Commercially available reagents were purchased and used without further purification unless otherwise indicated. Tetrahydrofuran and diethyl ether were distilled from purple solutions of benzophenone ketyl under nitrogen, and dichloromethane was dried over P_2O_5 and distilled immediately prior to use. Air-sensitive material was manipulated under a nitrogen atmosphere in a glove box or by standard Schlenk techniques. Aminopyridine ligands (**L1a**~**L1e**, **L2a**~**L2e**) were prepared accordingly to the method reported previously.[5h]

The IR spectra were recorded on a Bio-Rad FTS-40 spectrophotometer. The UV-Vis spectra were obtained by using a Hitachi U-3010 spectrophotometer. The NMR spectra were measured on a Bruker AC-300, and the corresponding frequencies for ^{13}C NMR spectra were 75.469 MHz. Values upfield of ^{1}H and ^{13}C data were given in δ (ppm) relative to chloroform in $CDCl_3$ (7.26, $CHCl_3$; 77.0, $CHCl_3$). Mass spectrometric analyses were collected on a JEOL SX-102A spectrometer or a Finnigan MAT 95S Spectrometer. Elemental analysis was done on a Perkin-Elmer 2400 CHN analyzer. Gel permeation chromatography (GPC) was performed in toluene at 40 °C using a Kratos model spectroflow 400 equipped with PL-mixed D exclusion limit 400k columns. Differential scanning calorimetry was measured under a continuous nitrogen purge (20 mL/min) on a Perkin-Elmer Pyris 6 DSC instrument. The data were gathered on the second heating cycle using a heating and cooling scan rate of 10 °C/min. Thermo-gravimetric analysis was carried out using a TA Instruments TGA5100 with a hating rate of 10 °C/min from 0 °C to 800 °C under a continuous nitrogen purge. Magnetic moments were measured between 2~300 K with an applied field up to 7 T, using a MPMS7 SQUID magnetometer (Quantum Design, USA). The morphologies of polyethylene were characterized by scanning electron microscope (SEM, JEOL JSM-6700F). Powder X-ray diffraction data were recorded on a Scintag X1 diffractometer using CuKα radiation (λ = 1.5426 Å) in the 2θ range 15-30°.

Synthesis and charaterization

Et_2NCH_2(*o*-C_6H_4N) (L1f) A mixture of 2-pyridinecarboxaldehyde (1.52 mL, 10 mmol), diethylamine (6.20 mL, 60 mmol), sodium borohydride (260 mg, 7 mmol) and 36% HCl solution (1.70 mL, 20 mmol) in MeOH (100 mL) was stirred at room temperature for 3 days. After removal of solvent, the resulting residue was neutralized with 0.1 M NaOH solution (10 mL) and extracted with Et_2O. The organic phase was concentrated by rota-vapor and purified by silica gel column chromatography using CH_2Cl_2 : MeOH (1 : 11, v/v) as elution solvent. The desired ligand **L1f** was obtained as a yellow liquid in 11 % yield

(200 mg). ^{1}H NMR (300 MHz, $CDCl_3$): δ 8.49 (d, J_{H-H} = 3.3 Hz, 1H, Py H-6), 7.61 (m, 1H, Py H-4), 7.44 (d, J_{H-H} = 7.7 Hz, 1H, Py H-3), 7.11 (m, 1H, Py H-5), 3.70 (s, 2H, Py-CH_2N), 2.55 (q, J_{H-H} = 7.1 Hz, 4H, N(CH_2CH$_3$)$_2$), 1.03 (t, J_{H-H} = 7.0 Hz, 6H, N(CH$_2$CH_3)$_2$). ^{13}C NMR (75.469 MHz, $CDCl_3$): δ 160.3 (Py C-2), 148.7 (Py C-6), 136.2 (Py C-4), 122.8 (Py C-3), 121.5 (Py C-5), 59.3 (Py-CH$_2$N), 47.1 (N(CH$_2$CH$_3$)$_2$), 11.6 (N(CH$_2$$CH_3$)$_2$). HR-MS (EI, m/z): 163.1238 (M^+).

6-methyl-2-pyridinecarboxaldehyde A mixture of 6-methyl-2-pyridinemethanol (1.00 g, 8.12 mmol) and MnO_2 (3.00 g, 34.51 mmol) in toluene was refluxed for 4 h. After cooling, the resulting mixture was filtered through celite and concentrated by reduced pressure to give a limpid liquid product in 71 % yield (0.57 g). ^{1}H NMR (300 MHz, $CDCl_3$): δ 10.03 (s, 1H, Py-CHO), 7.36 (d, J_{H-H} = 6.6 Hz, 1H, Py H-3), 7.25~7.21 (m, 2H, Py H-4, Py H-5), 2.64 (s, 3H, CH_3).

(2,6-^{i}Pr$_2$C$_6$H$_3$)HNCH$_2$(*o*-(6-Me)C$_6$H$_3$N) (L3e) A 50 mL solution of CH_2Cl_2 that contained 6-methyl-2-pyridinecarboxaldehyde (0.57 g, 4.70 mmol) and 2,6-diisopropylaniline (1.10 mL, 5.83 mmol) was refluxed in the presence of catalytic amounts of sulfuric acid and 4 A° activated molecular sieves for 4 h. After removal of solvent, excess $NaBH_4$ (0.70 g, 18.51 mmol) was added to the residue which dissolved in MeOH (100 mL). The reaction was stirred at room temperature for 1 day, then quenched by water and extracted into dichloromethane. Then the solvent was removed under reduced pressure to give a yellow liquid product **L3e** in 31% yield (0.58 g). ^{1}H NMR (300 MHz, $CDCl_3$): δ 7.51 (t, J_{H-H} = 7.5 Hz, 1H, Py H-4), 7.13~7.02 (m, 2H, Py H-3, Py H-5; 3H, Ph), 4.17 (s, 2H, Py-CH_2N), 3.40 (m, 2H, CH(CH$_3$)$_2$), 2.58 (s, 3H, Py-CH_3), 1.21 (d, J_{H-H} = 6.9 Hz, 12H, CH(CH_3)$_2$). ^{13}C NMR (75.469 MHz, $CDCl_3$): δ 158.0 (Py C-2), 157.8 (Py C-6), 143.4 (Py C-4), 142.5, 136.6, 123.6, 121.5 (Ph), 123.5, 118.8 (Py C-3, Py C-5), 56.5 (Py-CH$_2$N), 27.7 (CH(CH$_3$)$_2$), 24.5 (Py-CH$_3$), 24.2 (CH(CH$_3$)$_2$). HR-MS (EI, m/z): 282.2096 (M^+).

2-(2-pyridinyl)ethyl tosylate A mixture of 2-(2-hydroxyethyl) pyridine (2.80 mL, 25 mmol) and tosyl chloride (4.70 g, 25 mmol) in pyridine was stirred at 0 °C for 30 min. The solution was allowed to stand undisturbed at 4 °C overnight and precipitated by addition of ice/water mixtures. After filtration, the resulting solid was dried in vacuum to give a white product in 78% yield (5.43 g). ^{1}H NMR (300 MHz, $CDCl_3$): δ 8.40 (d, J_{H-H} = 4.2 Hz, 1H, Py H-6), 7.57 (m, 1H, Py H-5), 7.13 (m, 2H, Py H-3, Py H-4), 8.80~7.20 (m, 4H, Ph), 4.40 (t, J_{H-H} = 6.6 Hz, 2H, Py-CH_2CH$_2$N), 3.10 (t, J_{H-H} = 6.6 Hz, 2H, Py-CH$_2$CH_2N), 2.40 (s, 3H, Ph-CH_3).

^{i}PrHNCH$_2$CH$_2$(*o*-C$_6$H$_4$N) (L4a) A mixture of 2-(2-pyridinyl) ethyl tosylate (8.50 g, 30.5 mmol) and isopropylamine (7.70 mL, 87.5 mmol) in CH_2Cl_2 was refluxed for 24 h. The resulting mixture was washed with water and the organic phase was separated form the aqueous phase. The aqueous phase was extracted with CH_2Cl_2 again, and the organic phases were combined and neutralized with NaOH pellets. After filtration, the solvent was removed in vacuum to give a yellow liquid product **L4a** in 30% yield (1.50 g). ^{1}H NMR (300 MHz, $CDCl_3$): δ 8.51 (d, J_{H-H} = 4.8 Hz, 1H, Py H-6), 7.60 (m, 1H, Py H-5), 7.26 (d, J_{H-H} = 8.0 Hz, 1H, Py H-3), 7.12 (m, 1H, Py H-4), 2.97 (t, 4H, Py-CH_2CH$_2$N), 2.77 (q, J_{H-H} = 7.1 Hz, 2H, NCH(CH$_3$)$_2$), 1.12 (t, J_{H-H} = 6.0 Hz, 6H, NCH(CH_3)$_2$). ^{13}C NMR (75.469 MHz, $CDCl_3$): δ 160.1 (Py C-2), 149.1 (Py C-6), 136.1 (Py C-4), 123.1, 121.0 (Py C-3, Py C-5), 48.3 (Py-CH$_2$CH$_2$N), 46.8 (NCH(CH$_3$)$_2$), 38.6 (Py-CH$_2$$CH_2$N), 22.8 (NCH($CH_3$)$_2$). HR-MS (EI, m/z): 164.1307 (M^+).

^{t}BuHNCH$_2$CH$_2$(*o*-C$_6$H$_4$N) (L4b) The synthesis was carried out according to the same procedure as for **L4a**, using 2-(2-pyridinyl)ethyl tosylate (4.10 g, 14.8 mmol) and *tert*-butylamine (9.50 mL, 89.6 mmol) to give a yellow liquid **L4b** (0.47 g, 18%). ^{1}H NMR (300 MHz, $CDCl_3$): δ 8.44 (d, J_{H-H} = 4.0 Hz, 1H, Py H-6), 7.46 (m, 1H, Py H-5), 7.10 (d, J_{H-H} = 7.4 Hz, 1H, Py H-3), 7.02 (m, 1H, Py H-4), 2.87 (s, 4H, Py-CH_2CH_2N), 1.00 (s, 9H, NC(CH_3)$_3$). ^{13}C NMR (75.469 MHz, $CDCl_3$): δ 160.2 (Py C-2), 149.0 (Py C-6), 136.1 (Py C-4), 123.1, 121.0 (Py C-3, Py C-5), 55.3 (Py-CH$_2$CH$_2$N), 42.3 (NC(CH$_3$)$_3$), 39.1 (Py-CH$_2$$CH_2$N), 28.8 (NC($CH_3$)$_3$). HR-MS (EI, m/z): 178.1481 (M^+).

Et$_2$NCH$_2$CH$_2$(*o*-C$_6$H$_4$N) (L4f) The synthesis was carried out according to the same procedure as for **L4a**, using 2-(2-pyridinyl)ethyl tosylate (2.22 g, 8.0 mmol) and diethylamine (10.00 mL, 96.8 mmol) to give a yellow liquid **L4f** (0.53 g, 37%). ^{1}H NMR (300 MHz, $CDCl_3$): δ 8.49 (d, J_{H-H} = 4.2 Hz, 1H, Py H-6), 7.53 (m, 1H, Py H-5), 7.14 (d, J_{H-H} = 7.8 Hz, 1H, Py H-3), 7.07 (m, 1H, Py H-4), 2.83 (m, 2H, Py-CH_2CH$_2$N), 2.82 (m, 2H, Py-CH$_2$CH_2N), 2.57 (q, 4H, N(CH_2CH$_3$)$_2$), 1.02 (t, 6H, N(CH$_2$CH_3)$_2$). ^{13}C NMR (75.469 MHz, $CDCl_3$): δ 160.6 (Py C-2), 149.2 (Py C-6), 136.3 (Py C-4), 123.1, 121.1 (Py C-3, Py C-5), 55.7 (Py-CH$_2$CH$_2$N), 46.9 (N(CH$_2$CH$_3$)$_2$), 35.5 (Py-CH$_2$$CH_2$N), 11.7 (N(CH$_2CH_3$)$_2$). HR-MS (EI, m/z): 178.1473 (M^+).

[^{i}PrHNCH$_2$(*o*-C$_6$H$_4$N)]NiBr$_2$ (1a) To a stirred solution of (DME)$NiBr_2$ (230 mg, 0.73 mmol) in dried THF (20 mL) was added **L1a** (110 mg, 0.73 mmol) under N_2 atmosphere. The mixture was stirred at room temperature for 1 h. After concentration under vacuum, the residue was precipitated by addition of Et_2O (15 mL). The resulting suspension was filtered and dried under vacuum to give an air-sensitive yellowish-brown powder in 60% yield (170 mg). MS (FAB, m/z): 287.0, 289.0 (M^+-Br). UV-VIS (THF): $_{max}$ = 497.5 nm. Anal. Calcd. for $C_9H_{14}N_2NiBr_2$: C, 29.32; H, 3.83; N, 7.60. Found: C, 28.69; H, 4.15; N, 7.76.

[^{t}BuHNCH$_2$(*o*-C$_6$H$_4$N)]NiBr$_2$ (1b) The synthesis was carried out according to the same procedure as for **1a**, using (DME)$NiBr_2$ (300 mg, 0.96 mmol) and **L1b** (164 mg, 1.00 mmol) to give an air-sensitive purple product **1b** (230 mg, 60%). MS (FAB, m/z): 301.0, 303.0 (M^+-Br). UV-VIS (CH_2Cl_2): $_{max}$ = 498.5 nm. Anal. Calcd. for $C_{10}H_{16}N_2NiBr_2$: C, 31.38; H, 4.21; N, 7.32. Found: C, 31.12; H, 4.14; N, 7.14.

[PhHNCH$_2$(*o*-C$_6$H$_4$N)]NiBr$_2$ (1c) The synthesis was carried out according to the same procedure as for **1a**, using (DME)$NiBr_2$ (150 mg, 0.48 mmol) which dissolved in dried CH_2Cl_2 and **L1c** (90 mg, 0.49 mmol) to give an air-sensitive yellow product **1c**

(120 mg, 60%). MS (FAB, m/z): 321.0, 323.0 (M^+-Br). UV-VIS (CH_2Cl_2): $_{max}$ = 247.0, 209.5 nm.

[(2,6-$Me_2C_6H_3$)HNCH$_2$(*o*-C_6H_4N)]NiBr$_2$ (1d) The synthesis was carried out according to the same procedure as for **1c**, using (DME)$NiBr_2$ (180 mg, 0.57 mmol) and **L1d** (110 mg, 0.52 mmol) to give an air-sensitive orange product **1d** (180 mg, 82%). Single crystals suitable for X-ray diffraction were grown by slow diffusion of Et_2O into a saturated $CHCl_3$ solution of **1d**. MS (FAB, m/z): 349.0, 351.0 (M^+-Br). UV-VIS (CH_2Cl_2): $_{max}$ = 228.5, 262.0 nm.

[(2,6-^{i}Pr$_2C_6H_3$)HNCH$_2$(*o*-C_6H_4N)]NiBr$_2$ (1e) The synthesis was carried out according to the same procedure as for **1c**, using (DME)$NiBr_2$ (300 mg, 0.96 mmol) and **L1e** (268 mg, 1.00 mmol) to give an air-sensitive yellowish-brown product **1e** (270 mg, 57%). Single crystals suitable for X-ray diffraction were grown by slow diffusion of Et_2O into a saturated CH_2Cl_2 solution of **1e**. MS (FAB, m/z): 405.1, 407.1 (M^+-Br). UV-VIS (CH_2Cl_2): $_{max}$ = 450 nm.

[Et$_2$NCH$_2$(*o*-C_6H_4N)]NiBr$_2$ (1f) The synthesis was carried out according to the same procedure as for **1c**, using (DME)$NiBr_2$ (350 mg, 1.11 mmol) and **L1f** (186 mg, 1.13 mmol) to give an air-sensitive purple product **1f** (280 mg, 65%). Single crystals suitable for X-ray diffraction were grown by slow diffusion of Et_2O into a saturated CH_2Cl_2 solution of **1f**. MS (FAB, m/z): 301.0, 303.0 (M^+-Br). UV-VIS (CH_2Cl_2): $_{max}$ = 502.5 nm. Anal. Calcd. for $C_{10}H_{16}N_2NiBr_2$: C, 31.38; H, 4.21; N, 7.31. Found: C, 30.83; H, 4.45; N, 7.29.

[^{i}PrHNCMeH(*o*-C_6H_4N)]NiBr$_2$ (2a) The synthesis was carried out according to the same procedure as for **1c**, using (DME)$NiBr_2$ (300 mg, 0.96 mmol) and **L2a** (164 mg, 1.00 mmol) to give an air-sensitive light brown product **2a** (330 mg, 71%). Single crystals suitable for X-ray diffraction were grown by slow diffusion of Et_2O into a saturated CH_2Cl_2 solution of **2a**. MS (FAB, m/z): 301.0, 303.0 (M^+-Br). UV-VIS (CH_2Cl_2): $_{max}$ = 497.0, 651.0 nm. Anal. Calcd. for $C_{10}H_{16}N_2NiBr_2$: C, 31.38; H, 4.21; N, 7.31. Found: C, 30.35; H, 4.22; N, 7.22.

[PhHNCMeH(*o*-C_6H_4N)]NiBr$_2$ (2c) The synthesis was carried out according to the same procedure as for **1c**, using (DME)$NiBr_2$ (150 mg, 0.48 mmol) and **L2c** (85 mg, 0.43 mmol) to give an air-sensitive yellowish-brown product **2c** (160 mg, 80%). MS (FAB, m/z): 334.9, 336.9 (M^+-Br). UV-VIS (THF): $_{max}$ = 494.0 nm.

[(2,6-$Me_2C_6H_3$)HNCMeH(*o*-C_6H_4N)]NiBr$_2$ (2d) The synthesis was carried out according to the same procedure as for **1c**, using (DME)$NiBr_2$ (200 mg, 0.64 mmol) and **L2d** (110 mg, 0.49 mmol) to give an air-sensitive orange product **2d** (190 mg, 86%). Single crystals suitable for X-ray diffraction were grown by slow diffusion of Et_2O into a saturated $CHCl_3$ solution of **2d**. MS (FAB, m/z): 363.0, 365.0 (M^+-Br). Anal. Calcd. for $C_{15}H_{18}N_2NiBr_2$: C, 40.50; H, 4.08; N, 6.30. Found: C, 40.29; H, 4.15; N, 6.30.

[(2,6-^{i}Pr$_2C_6H_3$)HNCMeH(*o*-C_6H_4N)]NiBr$_2$ (2e) The synthesis was carried out according to the same procedure as for **1c**, using (DME)$NiBr_2$ (150 mg, 0.48 mmol) and **L2e** (71 mg, 0.25 mmol) to give an air-sensitive orange product **2e** (90 mg, 75%). Single crystals suitable for X-ray diffraction were grown by slow diffusion of Et_2O into a saturated CH_2Cl_2 solution of **2e**. MS (FAB, m/z): 419.0, 421.0 (M^+-Br). UV-VIS (CH_2Cl_2): $_{max}$ = 464.6 nm.

[(2,6-^{i}Pr$_2C_6H_3$)HNCH$_2$(*o*-(6-Me)C_6H_3N)]NiBr$_2$ (3e) The synthesis was carried out according to the same procedure as for **1c**, using (DME)$NiBr_2$ (150 mg, 0.48 mmol) and **L3e** (141 mg, 0.50 mmol) to give an air-sensitive yellow product **3e** (140 mg, 56%). Single crystals suitable for X-ray diffraction were grown by slow diffusion of Et_2O into a saturated CH_2Cl_2 solution of **3e**. MS (FAB, m/z): 419.1, 421.1 (M^+-Br). UV-VIS (CH_2Cl_2): $_{max}$ = 497.5 nm.

[^{i}PrHNCH$_2$CH$_2$(*o*-C_6H_4N)]NiBr$_2$ (4a) The synthesis was carried out according to the same procedure as for **1c**, using (DME)$NiBr_2$ (150 mg, 0.48 mmol) and **L4a** (82 mg, 0.50 mmol) to give an air-sensitive purple product **4a** (110 mg, 65%). Single crystals suitable for X-ray diffraction were grown by slow diffusion of pentane into a saturated CH_2Cl_2 solution of **4a**. MS (FAB, m/z): 301.0, 303.0 (M^+-Br). UV-VIS (CH_2Cl_2): $_{max}$ = 525 nm. Anal. Calcd. for $C_{10}H_{16}N_2NiBr_2$: C, 31.38; H, 4.21; N, 7.31. Found: C, 30.17; H, 4.94; N, 8.02.

[^{t}BuHNCH$_2$CH$_2$(*o*-C_6H_4N)]NiBr$_2$ (4b) The synthesis was carried out according to the same procedure as for **1c**, using (DME)$NiBr_2$ (150 mg, 0.48 mmol) and **L4b** (89 mg, 0.50 mmol) to give an air-sensitive purple product **4b** (80 mg, 42%). Single crystals suitable for X-ray diffraction were grown by slow diffusion of Et_2O into a saturated CH_2Cl_2 solution of **4b**. MS (FAB, m/z): 315.1, 317.1 (M^+-Br). UV-VIS (CH_2Cl_2): $_{max}$ = 522 nm.

[Et$_2$NCH$_2$CH$_2$(*o*-C_6H_4N)]NiBr$_2$ (4f) The synthesis was carried out according to the same procedure as for **1c**, using (DME)$NiBr_2$ (150 mg, 0.48 mmol) and **L4f** (90 mg, 0.50 mmol) to give an air-sensitive purple product **4f** (60 mg, 31%). Single crystals suitable for X-ray diffraction were grown by slow diffusion of Et_2O into a saturated CH_2Cl_2 solution of **4f**. MS (FAB, m/z): 315.0, 317.0 (M^+-Br). UV-VIS (CH_2Cl_2): $_{max}$ = 533 nm.

[^{i}PrHNCH$_2$(*o*-C_6H_4N)]$_2$NiBr$_2$ (1a') The synthesis was carried out according to the same procedure as for **1c**, using (DME)$NiBr_2$ (300 mg, 0.96 mmol) and **L1a** (300 mg, 2.00 mmol) to give an air-sensitive green product **1a'** (371 mg, 74%). Single crystals suitable for X-ray diffraction were grown by slow diffusion of Et_2O into a saturated CH_2Cl_2 solution of **1a'**. MS (FAB, m/z): 439.1, 437.1 (M^+-Br). UV-VIS (CH_2Cl_2): $_{max}$ = 402.5, 489.0, 664 nm.

[^{t}BuHNCH$_2$(*o*-C_6H_4N)]$_2$NiBr$_2$ (1b') The synthesis was carried out according to the same procedure as for **1c**, using (DME)$NiBr_2$ (300 mg, 0.96 mmol) and **L1b** (328 mg, 2.00 mmol) to give an air-sensitive green product **1b'** (250 mg, 48%). Single crystals suitable for X-ray diffraction were grown by slow diffusion of Et_2O into a saturated CH_2Cl_2 solution of **1b'**. MS (FAB, m/z): 467.1, 465.1 (M^+-Br). UV-VIS (CH_2Cl_2): $_{max}$ = 402.5, 492.0, 658.5 nm.

[(2,6-$Me_2C_6H_3$)HNCH$_2$(*o*-C_6H_4N)]$_2$NiBr$_2$ (1d') The synthesis was carried out according to the same procedure as for **1c**, using

(DME)$NiBr_2$ (300 mg, 0.96 mmol) and **L1d** (424 mg, 2.00 mmol) to give an air-sensitive green product **1d'** (510 mg, 83%). Single crystals suitable for X-ray diffraction were grown by slow diffusion of Et_2O into a saturated CH_2Cl_2 solution of **1d'**. MS (FAB, m/z): 563.1, 561.1 (M^+-Br). UV-VIS (CH_2Cl_2): $_{max}$ = 644.5 nm.

General Procedure for Polymerization of Ethylene

Into a 600 mL of Parr autoclave equipped with a magnetic stirring bar was placed the nickel complexes (8-10 mg), MAO (3-12 mL) and dried toluene (50-200 mL) in glovebox. The autoclave was sealed and took out from glovebox. Upon flushed with ethylene gas for several times, ethylene gas was pressurized (14-21 bar). The mixture was stirred for a period of time with constant pressure of ethylene was during the polymerization runs. The reaction was quenched with venting the autoclave followed by addition of methanol/HCl (10:1). Toluene was used to extract the organic, and methanol or acetone was to precipitate the PE.

In a typical run, to a 600 mL autoclave was placed 20 μmol of the catalyst and 5 mL of MAO (10 wt%) in 50 mL of predried toluene. The thermostated autoclave was sealed and flushed several times with ethylene. Ethylene then was pressurized up to 17 bar. The reaction ran for 2h at 25 °C, then quenched by venting the autoclave followed by adding 100 mL of methanol/HCl in 10:1 v/v ratio. After stirring for 30 minutes, the organic was extracted into toluene and concentrated under vacuum. The residue was precipitated by addition of large amount of acetone, and the resulting polymers were filtered and dried in vacuo. The GPC analysis was done to the soluble part in toluene solutions, relative to polystyrene standards.

X-ray crystallographic Analysis

Diffraction data were measured on a Nonius CAD-4, SmartCCD, or Nonius KappaCCD diffractometer with graphite-monochromatized Mo K_α radiation (λ = 0.7103 Å). No significant decay was observed during the data collection. The data were processed on a PC using the SHELXTL refinement software package.[16] The structures were solved using the direct method and refined by full-matrix least-squares on the F^2 value.

All the non-hydrogen atoms were refined anisotropically. Hydrogen atoms were identified by calculation and refined using a riding mode, and their contributions to structure factors were included. Atomic scattering factors were taken from the International Tables of Crystallographic Data, Vol IV. Computing programs are from the NRC VAX package.[17] Crystallographic data and selected atomic coordinates and bond parameters are collected in Tables 4-5. The rest of data are supplied in the supplementary material.

Acknowledgements

We thank the National Science Council, Taiwan ROC, for the financial support, and also thank Nan-Ya Plastic Co. for the generous supply of MAO.

References

[a] Department of Chemistry, National Taiwan University, No 1, Section 4, Roosevelt Road, Taipei, Taiwan, 106, Tel: 8862-3366-1659, Fax: 8862-2363-6359, jtchen@ntu.edu.tw

Table 4 X-ray crystal parameters and data collection

Compound	1d'	1e	2a	4b
Formula	$C_{28}H_{32}Br_2N_4Ni$	$C_{36}H_{46}Br_4N_4Ni_2$	$[C_{10}H_{16}Br_2N_2Ni]_n$	$C_{11}H_{18}Br_2N_2Ni$
Formula wt	643.11	971.83	382.78	396.80
Crystal size / mm	0.40×0.35×0.35	0.22×0.20×0.20	0.42×0.25×0.25	0.30×0.30×0.25
Crystal system	Monoclinic	Monoclinic	Monoclinic	Monoclinic
Space group	*C*2/c	$P2_1/n$	$P2_1/c$	$P2_1/c$
a / Å	28.5705(7)	12.8652(1)	6.7101(3)	13.9446(5)
b / Å	15.3292(4)	10.1571(1)	15.5170(7)	8.1918(3)
c / Å	14.9325(4)	14.6983(2)	12.6527(6)	13.5562(4)
α / °	90	90	90	90
β / °	120.6625(5)	104.6604(5)	94.437(1)	108.2726(7)
γ / °	90	90	90	90
V / Å^3	5625.5(3)	1858.14(3)	1313.5(1)	1470.46(9)
Z	8	2	4	4
ρ_{calcd} / Mg·m^{-3}	1.519	1.737	1.936	1.792
F(000)	2608	972	752	784
T / K	295(2)	150(2)	295(2)	295(2)
μ / mm^{-1}	3.554	5.345	7.533	6.732
Transmission	0.4210-0.4915	0.360-0.319	0.2292-0.4915	0.3791-0.4915
θ range / °	1.57~27.50	1.88~27.50	2.08~27.50	1.54~27.50
h, *k*, *l*	±37, ±19, -19~18	±16, -12~13, -19~18	-7~8, ±20, ±16	±18, ±10, ±17
Reflections collected	29520	15027	11726	13160
Independent reflections	6454	4263	3008	3374
R_{int}	0.0371	0.0350	0.0358	0.0294
Data / restraints	6454/0	4263/0	3008/0	3374/0
Parameters	316	213	137	145
R_1 [I>2σ(I)]	0.0328	0.0357	0.0232	0.0382
wR_2 [I>2σ(I)]	0.0776	0.0883	0.0463	0.1141
R_1 (all data)	0.0711	0.0493	0.0375	0.0609
wR_2 (all data)	0.0842	0.1012	0.0486	0.1223
Goodness of fit on F^2	1.016	1.225	1.009	1.027
Largest diff. peak and hole eÅ^{-3}	0.464 and -0.379	0.836 and -0.683	0.388 and -0.361	0.861 and -1.059

Table 5 Selected bond distances (Å) and angles (°)

[(2,6-$Me_2C_6H_3$)$HNCH_2$(*o*-C_6H_4N)]$_2NiBr_2$ (**1d'**)							
Ni-N1	2.030 (2)	Ni-N2	2.122 (2)	Ni-Br1	2.4235 (5)	N1-C5	1.333 (4)
N2-C6	1.489 (4)	C5-C6	1.504 (4)	N2-C7	1.465 (4)		
N1-Ni-N2	81.58 (9)	Ni-N1-C5	116.8 (2)	Ni-N2-C6	110.5 (2)	N1-C5-C6	117.8 (3)
N2-C6-C5	112.9 (3)	N1-Ni-N3	172.7 (1)	N2-Ni-Br1	133.51 (7)	N2-Ni-N4	102.4 (1)
N4-Ni-Br1	124.07 (7)	C7-N2-Ni	113.2 (2)				
[(2,6-$^i Pr_2C_6H_3$)$HNCH_2$(*o*-C_6H_4N)]$NiBr_2$ (**1e**)							
Ni-N1	2.026 (3)	Ni-N2	2.122 (3)	Ni-Br1	2.4882(5)	Ni-Br2	2.4229 (5)
Ni-Br1A	2.5512 (5)	N1-C5	1.341 (4)	N2-C6	1.479 (4)	C5-C6	1.502 (4)
N2-C7	1.474 (4)						
N1-Ni-N2	81.1 (1)	Ni-N1-C5	116.8 (2)	Ni-N2-C6	109.8 (2)	N1-C5-C6	115.7 (3)
N2-C6-C5	111.9 (2)	N1-Ni-Br1	168.39 (8)	N2-Ni-Br2	140.32 (8)	N2-Ni-Br1A	99.94 (8)
Br2-Ni-Br1A	119.16 (2)	Br1-Ni-Br1A	86.48 (2)	Ni-Br1-Ni1A	93.52 (2)	C7-N2-Ni	125.0 (2)
{[^{i}PrHNCMeH(*o*-C_6H_4N)]$NiBr_2$}$_n$ (**2a**)							
Ni-N1	2.049 (2)	Ni-N2	2.124 (2)	Ni-Br1	2.5958 (4)	Ni-Br2	2.6052 (4)
Ni-Br1A	2.6221 (4)	Ni-Br2B	2.6087 (4)	N1-C5	1.335 (3)	N2-C6	1.484 (3)
C5-C6	1.511 (4)	N2-C8	1.495 (3)				
N1-Ni-N2	80.21 (9)	Ni-N1-C5	116.3 (2)	Ni-N2-C6	111.9 (2)	N1-C5-C6	118.3 (2)
N2-C6-C5	109.7 (2)	Br1-Ni-Br2	93.17 (1)	N1-Ni-Br1	167.16 (7)	N2-Ni-Br2	178.58 (6)
Br1A-Ni-Br2B	169.81 (2)	C8-N2-Ni	118.5 (2)	Br1-Ni-Br1A	85.52 (1)	Ni-Br1-NiA	94.48 (1)
Br2-Ni-Br2B	81.54 (1)	Ni-Br2-NiB	98.46 (1)				
[^{t}BuHNCH$_2$CH$_2$(*o*-C_6H_4N)]$NiBr_2$ (**4b**)							
Ni-N1	1.991 (3)	Ni-N2	2.037 (3)	Ni-Br1	2.3728 (7)	Ni-Br2	2.3462 (7)
N1-C5	1.344 (5)	N2-C7	1.487 (5)	C5-C6	1.522 (6)	C6-C7	1.508 (6)
N2-C8	1.516 (5)						
N1-Ni-N2	98.5 (1)	Ni-N1-C5	121.6 (3)	Ni-N2-C7	113.9 (2)	N1-C5-C6	117.3 (4)
N2-C7-C6	112.3 (4)	C5-C6-C7	112.9 (4)	Br1-Ni-Br2	117.55 (3)	N1-Ni-Br1	106.6 (1)
N1-Ni-Br2	105.7 (1)	N2-Ni-Br1	98.14 (9)	N2-Ni-Br2	127.46 (9)	C8-N2-Ni	114.8 (3)

§ This article is dedicated to Prof. Dr. Christian Bruneau, University of Renne 1, on the occasion of his 60th birthday.

† Electronic Supplementary Information (ESI) available: [The SQUID data of **1d**, **1e**, **1f**, **2d**, **3e**, powder X-ray diffraction patterns and SEM images of polyethylene, ORTEP drawings and crystallographic data of **1a'**, **1b'**, **1d**, **1f**, **2d**, **2e**, **3e**, **4a**, **4f** are provided.

‡ This manuscript is mainly based on the M.S. thesis of Dr. Ya-Chi Lin, 2001.

1. (a) S. Mecking, *Angew. Chem. Int. Ed.,* 2001, **40**, 534-540; (b) V. C. Gibson and S. K. Spitzmesser, *Chem. Rev.*, 2003, **103**, 283-315; (c) J. Zhang, X. Wang and G.-X. Jin, *Coord. Chem. Rev.,* 2006, **250**, 95-109; (d) A. Michalak and T. Ziegler, *Kinet. Catal.*, 2006, **47**, 310-325; (e) B. K. Bahuleyan, D.-W. Park, C.-S. Ha and I. Kim, *Catal. Surv. Asia*, 2006, **10**, 65-73; (f) R. Hoff and R. T. Mathers, *Handbook of Transition Metal Polymerization Catalysts,* Wiley-VCH, Weinheim 2010, 459-466.
2. (a) S. D. Ittel, L. K. Johnson and M. Brookhart, *Chem. Rev.* 2000, **100**, 1169-1203; (b) W.-H. Sun, D. Zhang, S. Zhang, S. Jie, and J. Hou, *Kinet. Catal.*, 2006, **47**, 278-283; (c) Z. Guan and C. S. Popeney, *Top. Organomet. Chem.,* 2009, **26**, 179-220.
3. F.-Z. Yang, Y.-C. Chen, Y.-F. Lin, K.-H. Yu, Y.-H. Liu, Y. Wang, S.-T. Liu and J.-T. Chen, *Dalton Trans.*, 2009, 1243-1250.
4. (a) Z.-F. Huang, H.-Y. Gao, L. Zhang and Q. Wu, *Chin. J. Polym. Sci.,* 2008, **26**, 567-573; (b) Z.-F. Huang, K. Song, F.-S. Liu, J. Long, H. Hu, H.-Y. Gao and Q. Wu, *J. Polym. Sci. Part A: Polym. Chem.*, 2008, **46**, 1618-1628; (c) S. Zai, F.-S. Liu, H.-Y. Gao, C. Li, G.-Y. Zhou, S. Cheng, L.-H. Guo, L. Zhang, F.-M. Zhua and Q. Wu, *Chem. Commun*., 2010, **46**, 4321-4323.
5. (a) B. T. Cho and S. K. Kang, *Tetrahedron*, 2005, **61**, 5725-5734; (b) A. Raja, V. Rajendiran, P. U. Maheswari, R. Balamurugan, C. A. Kilner, M. A. Halcrow and M. Palaniandavar, *J. Inorg. Biochem*., 2005, **99**, 1717-1732; (c) V. Diez, J. V. Cuevas, G. García-Herbosa, G. Aullón, J. P. H. Charmant, A. Carbayo and A. Muñoz, *Inorg. Chem.*, 2007, **46**, 568-577; (d) S. J. Dickson, M. J. Paterson, C. E. Willans, K. M. Anderson and J. W. Steed, *Chem. Eur. J.,* 2008, **14**, 7296-7305; (e) V. V. Kouznetsov, L. Y. V. Méndez, M. Sortino, Y. Vásquez, M. P. Gupta, M. Freile, R. D. Enriz and S. A. Zacchino, *Bioorg. Med. Chem.*, 2008, **16**, 794-809; (f) G. Li, X. Qian, S. Yan, J. Cui, R. Zhang and Y. Xiao, *Monat. für Chemie*, 2008, **139**, 169-178; (g) K. Nienkemper, G. Kehr, S. Kehr, R. Fröhlich and G. Erker, *J. Organomet. Chem.,* 2008, **693**, 1572-1589; (h) Y.-C. Lin, K.-H. Yu, S.-L. Huang, Y.-H. Liu, Y. Wang, S.-T. Liu and J.-T. Chen, Dalton Trans., 2009, 9058-9067; (i) L. Annunziata, G. Li and C. Pellecchia, *J. Mol. Cat. A: Chem*., 2011, **337**, 1-8; (j) L. Annunziata, S. Pragliola, D. Pappalardo, C. Tedesco and C. Pellecchia, *Macromolecules,* 2011, **44**, 1934-1941.
6. R. F. Borch, M. D. Bernstein and H. D. Durst, *J. Am. Chem. Soc.*, 1971, **93**, 2897-2904.
7. (a) E. V. Rybak-Akimova, A. Y. Nazarenko, L. Chen, P. W. Krieger, A. M. Herrera, V. V. Tarasov and P. D. Robinson, *Inorg. Chim. Acta* 2001, **324**, 1-15; (b) K. Cheng, I. J. Kim, M.-J. Lee, S. A. Adah, T. J. Raymond, E. J. Bilsky, M. D. Aceto, E. L. May, L. S. Harris, A. Coop, C. M. Dersch, R. B. Rothman, A. E. Jacobson and K. C. Rice, *Org. Biomol. Chem.*, 2007, **5**, 1177-1190.
8. (a) D. P. Gates, S. A. Svejda, E. Oñate, C. M. Killian, L. K. Johnson, P. S. White and M. Brookhart, *Macromolecules*, 2000, **33**, 2320-2334; (b) R. J. Maldanis, J. S. Wood, A. Chandrasekaran, M. D. Rausch and J. C.W. Chien, *J. Organomet. Chem.,* 2002, **645**, 158-167; (c) H. S. Schrekker, V. Kotov, P. Preishuber-Pflugl, P. White and M. Brookhart, *Macromolecules*, 2006, **39**, 6341-6354.
9. (a) M. A. Jalil, S. Fujinami, H. Senda and H. Nishikawa, *J. Chem. Soc., Dalton Trans*., 1999, 1655–1661; (b) T. V. Laine, K. Lappalainen, J. Liimatta, E. Aitola, B. Löfgren and M. Leskelä, *Macromol. Rapid Commun.*, 1999, **20**, 487-491;

(c) T. V. Laine, U. Piironen, K. Lappalainen, M. Klinga, E. Aitola and M. Leskelä, *J. Organomet. Chem.*, 2000, **606**, 112-124; (d) W.-H. Sun, Z. Li, H. Hu, B. Wu, H. Yang, N. Zhu, X. Leng and H. Wang, *New J. Chem*., 2002, **26**, 1474-1478; (e) F. Speiser, P. Braunstein, L. Saussine and R. Welter, *Inorg. Chem.,* 2004, **43**, 1649-1658; (f) F. Speiser, P. Braunstein, L. Saussine and R. Welter, *Organometallics*, 2004, **23**, 2613-2624; (g) H.-R. Liu, P. T. Gomes, S. I. Costa, M. T. Duarte, R. Branquinho, A. C. Fernandes, J. C.W. Chien, R. P. Singh and M. M. Marques, *J. Organomet. Chem.*, 2005, **690**, 1314-1323; (h) A. Kermagoret and P. Braunstein, *Organometallics*, 2008, **27**, 88-99.

10. (a) M. A. Fox, D. A. Chandler and P.-W. Wang, *Macromolecules*, 1991, **24**, 4626-4636; (b) T. Suzuki, A. Morikawa and K. Kashiwabara, *Bull. Chem. Soc. Jpn.*, 1996, **69**, 2539-2548; (c) F. Li, G. P. A. Yap, S. L. Scott and S. I. Woo, *Transit. Met. Chem*., 2001, **26**, 271-275; (d) G. J. P. Britovsek, S. P. D. Baugh, O. Hoarau, V. C. Gibson, D. F. Wass, A. J. P. White and D. J. Williams, *Inorg. Chim. Acta*, 2003, **345**, 279-291.
11. Y. Fujii, *Bull. Chem. Soc. Jpn.*, 1970, **43**, 2815-2820.
12. (a) L. K. Johnson, C. M. Killian and M. Brookhart, *J. Am. Chem. Soc.*, 1995, **117**, 6414-6415; (b) M. Schmid, R. Eberhardt, M. Klinga, M. Leskelä and B. Rieger, *Organometallics*, 2001, **20**, 2321-2330; (c) M. D. Leatherman, S. A. Svejda, L. K. Johnson and M. Brookhart, *J. Am. Chem. Soc.*, 2003, **125**, 3068-3081; (d) D. Meinhard, M. Wegner, G. Kipiani, A. Hearley, P. Reuter, S. Fischer, O. Marti and B. Rieger, *J. Am. Chem. Soc.*, 2007, **129**, 9182-9191.
13. (a) S. Matsui and T. Fujita, *Catal. Today*, 2001, **66**, 63-73; (b) T. S. Seo, D. S. Hong, D. W. Jung, H. Y. Cho and S. I. Woo, *Korean J. Chem. Eng.*, 2002, **19**, 622-626; (c) G. J. P. Britovsek, S. P. D. Baugh, O. Hoarau, V. C. Gibson, D. F. Wass, A. J. P. White and D. J. Williams, *Inorg. Chim. Acta*, 2003, **345**, 279-291.
14. (a) S. A. Svejda and M. Brookhart, *Organometallics*, 1999, **18**, 65-74; (b) L. Chen, J. Hou and W.-H. Sun, Appl. Catal. A: Gen., 2003, **246**, 11-16.
15. (a) M. E. Vickers and H. Fischer, *Polymer*, 1995, **36**, 2667-2670; (b) Z. Bartczak, A. Galeski, A. S. Argon and R. E. Cohen, *Polymer*, 1996, **37**, 2113-2123; (c) K. E. Russell, B. K. Hunter and R. D. Heyding, *Polymer*, 1997, **38**, 1409-1414; (d) Y. L. Joo, O. H. Han, H.-K. Lee and J. K. Song, *Polymer*, 2000, **41**, 1355-1368; (e) A. M. E. Baker and A. H. Windle, *Polymer*, 2001, **42**, 667-680.
16. G. M. Sheldrick, SHELXTL-97, Program for Crystal Structure Solution, University of Göttingen, Germany, 1997.
17. D. T. Cromer and J. T. Waber, International Tables for X-ray Crystallography, The Kynoch Press, Birmingham, England, 1974, Vol. IV.

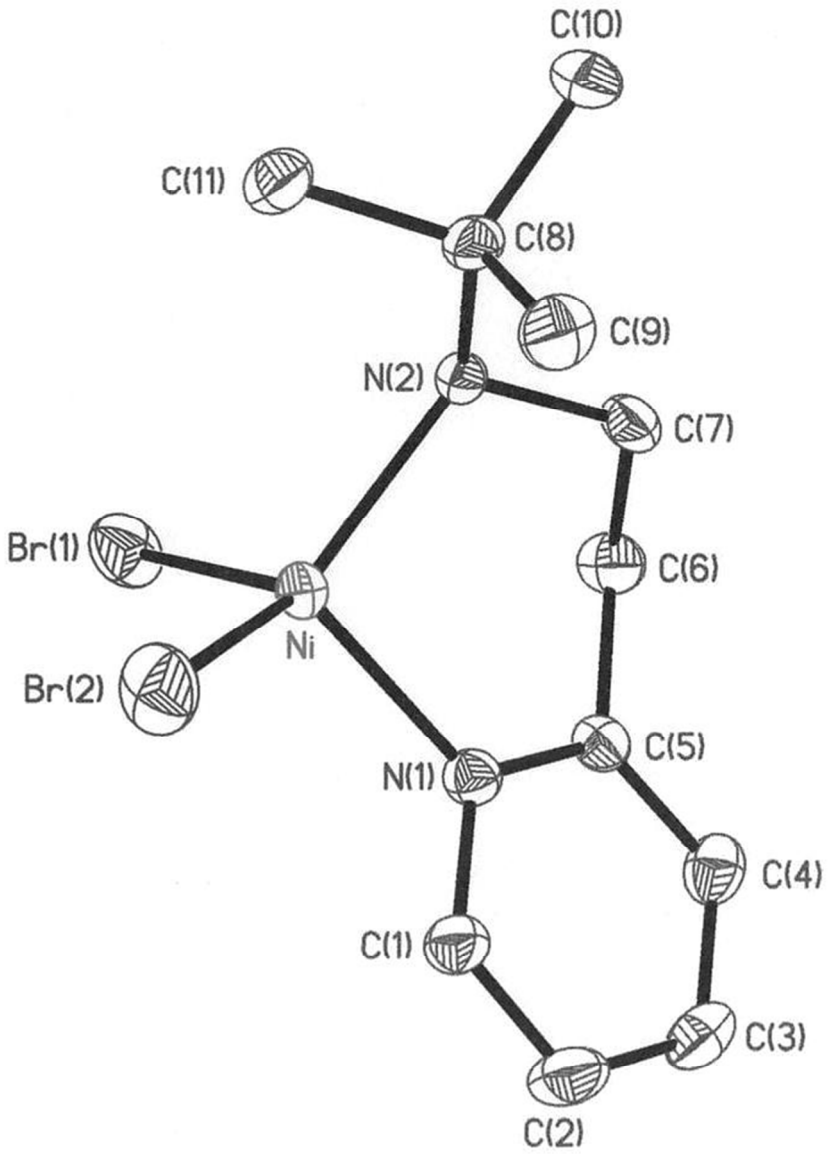

194x260mm (96 x 96 DPI)

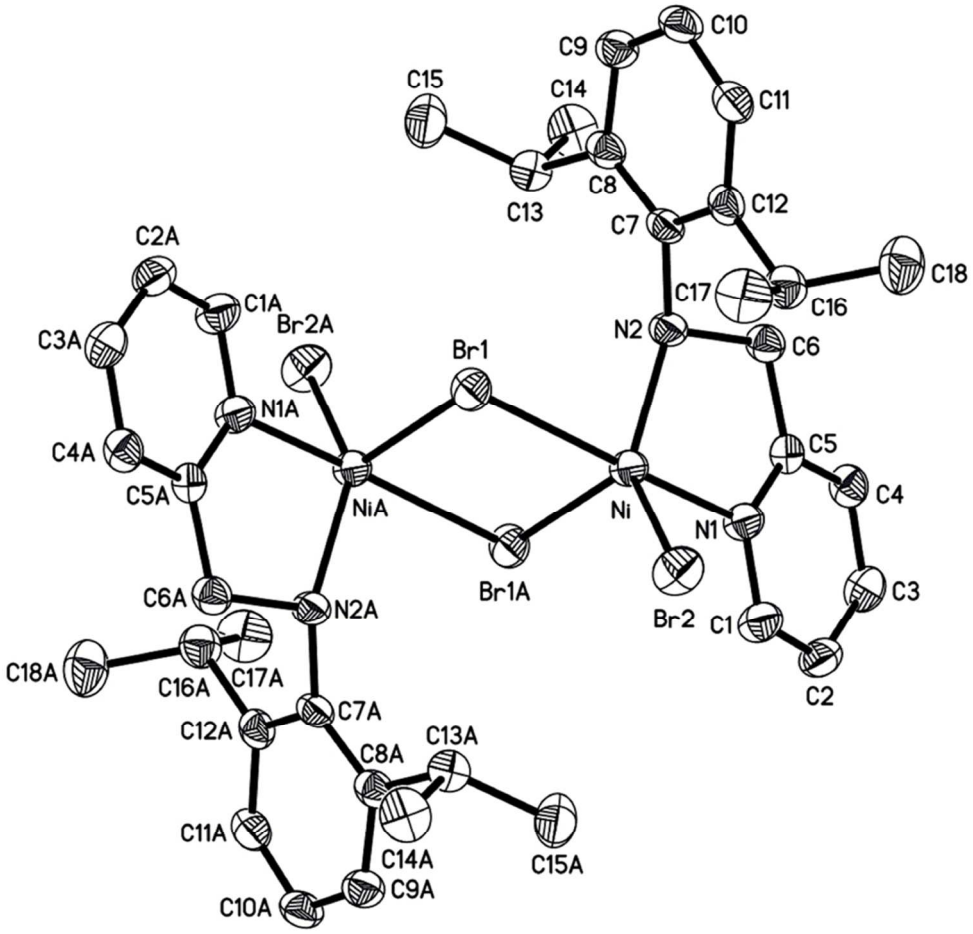

87x83mm (300 x 300 DPI)

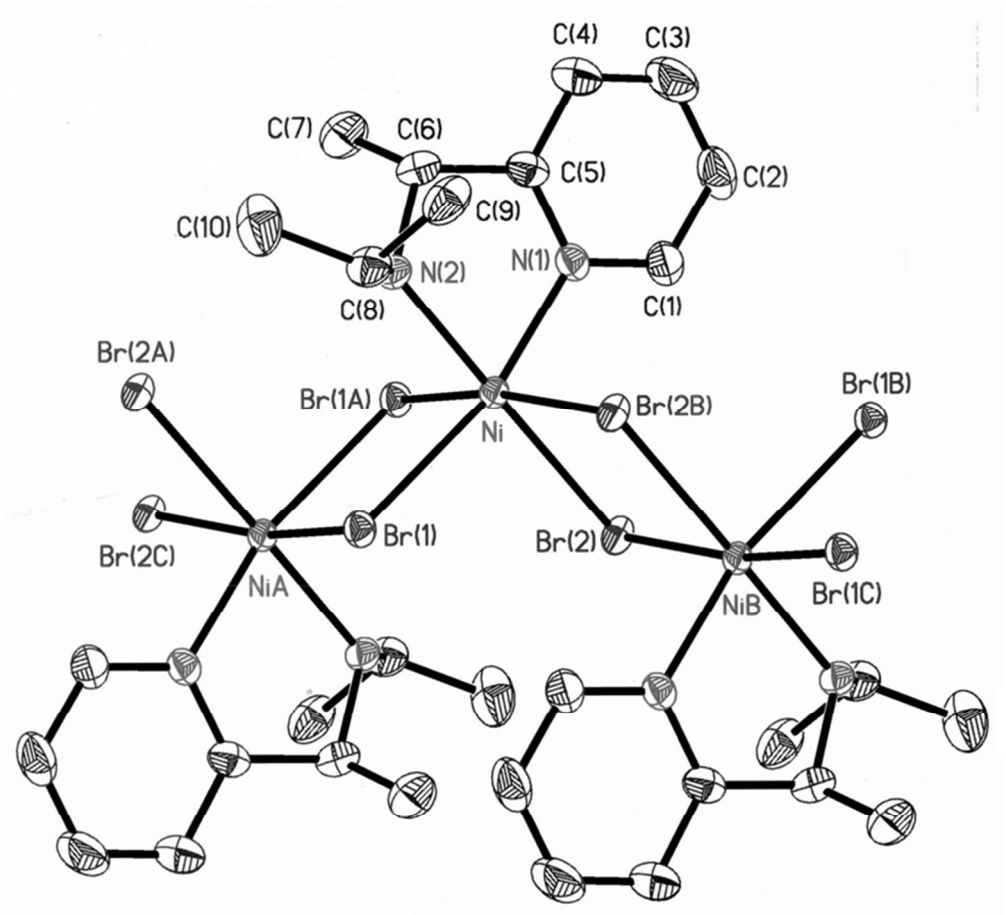

236x214mm (96 x 96 DPI)

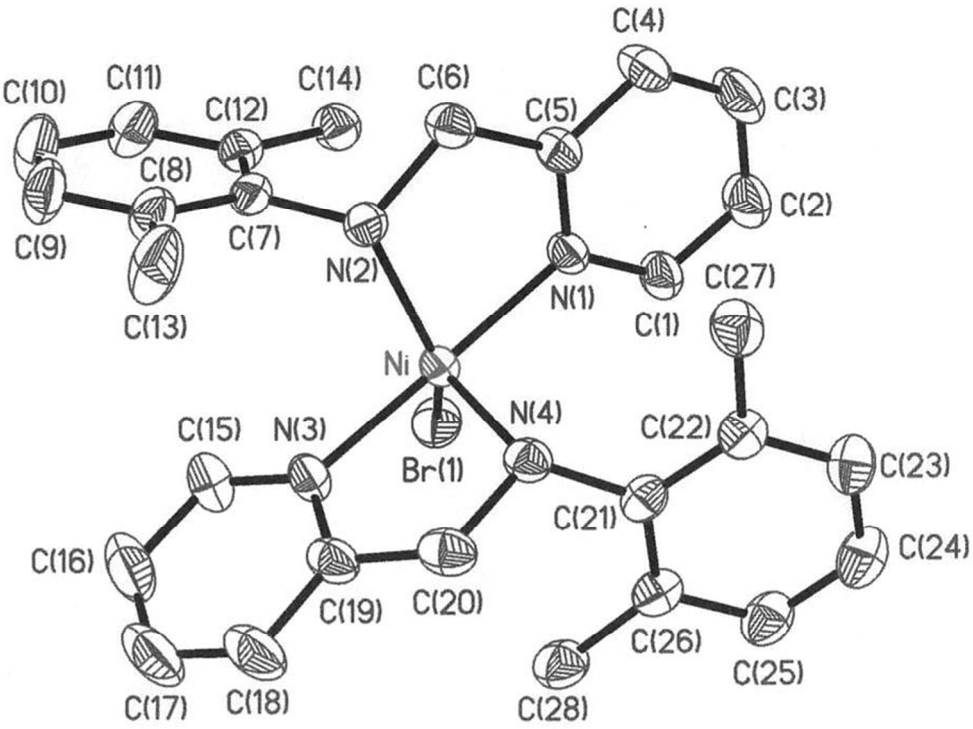

248x184mm (96 x 96 DPI)

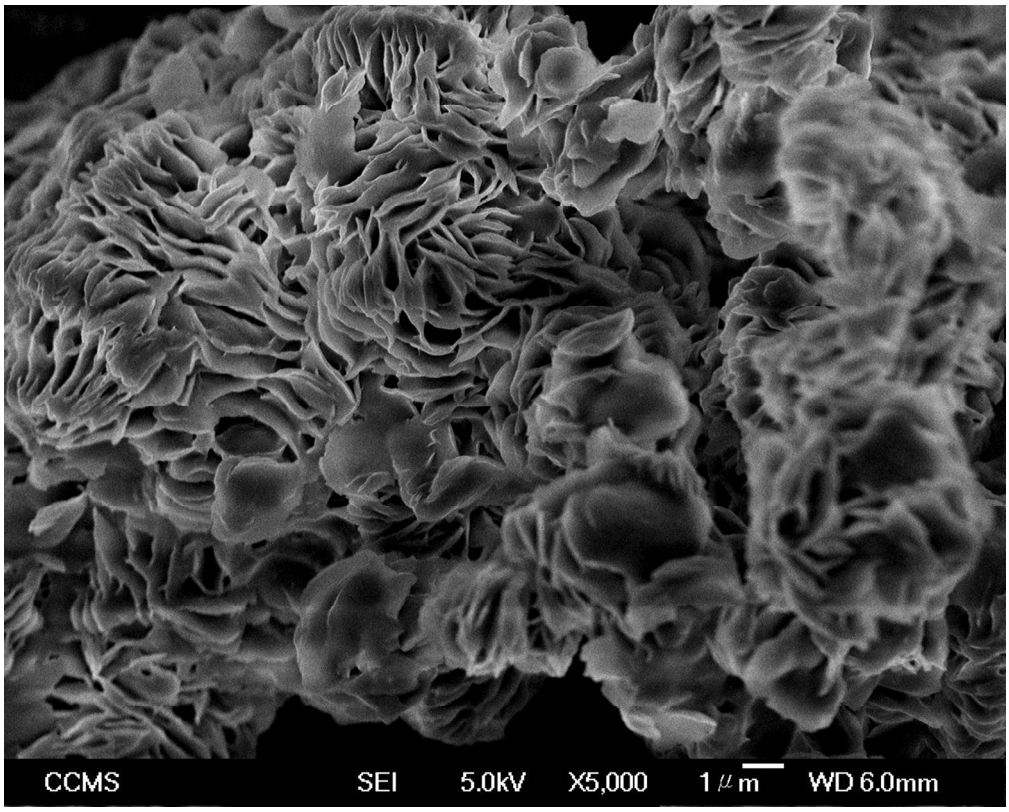

338x270mm (96 x 96 DPI)

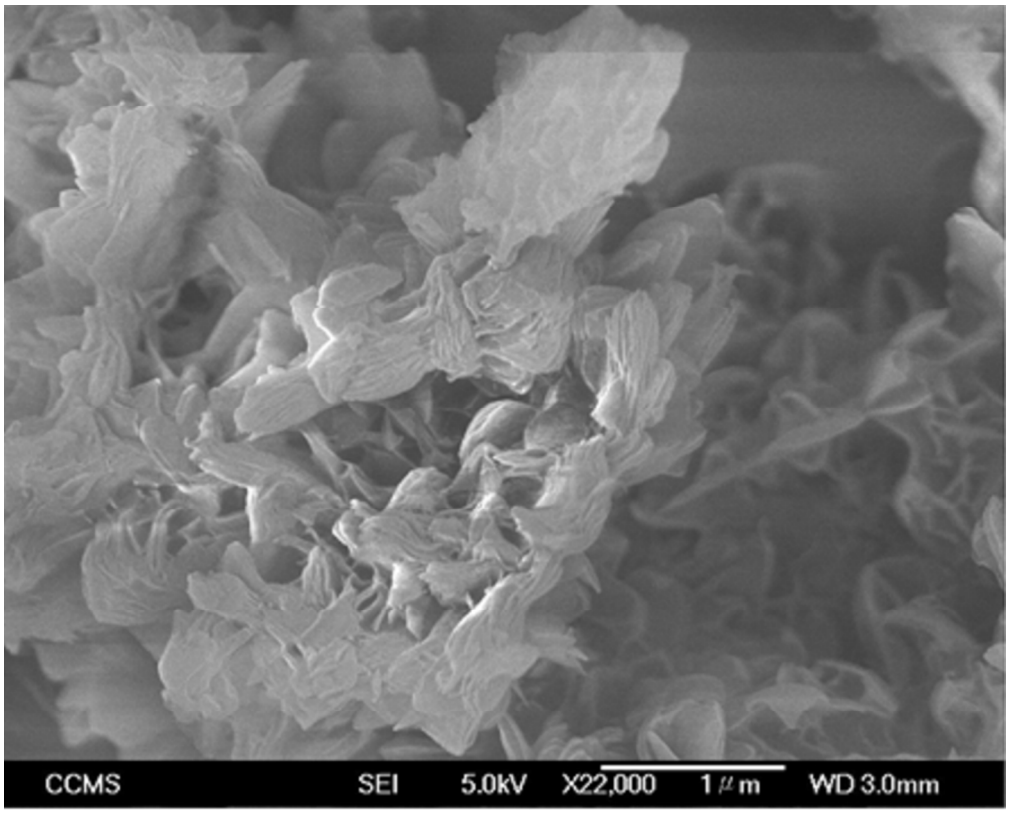

237x190mm (96 x 96 DPI)

Table of Content

Four structural configurations in (aminopyridine)$NiBr_2$ which are found to catalyze ethylene polymerization under mild conditions with the activity reaching 10^5 g PE/mol Ni·h are characterized.